Journal of Alloys and Compounds 498 (2010) 5–12

Contents lists available at ScienceDirect

Journal of Alloys and Compounds

journal homepage: www.elsevier.com/locate/jallcom

Cr_3Si doped by Co studied by muon spin relaxation and scanning electron microscopy techniques

P. Zaleski[a,*], K. Szymański[a], J. Przewoźnik[b], K. Rećko[a], S. Cottrell[c], L. Dobrzyński[a,d]

[a] Faculty of Physics, University of Białystok, Lipowa 41, 15-424 Białystok, Poland
[b] Faculty of Physics and Applied Computer Science, University of Mining and Metallurgy, Mickiewicza 30, 30-052 Cracow, Poland
[c] ISIS Facility, Rutherford Appleton Laboratory, Chilton, Didcot OX11 0QX, UK
[d] The Andrzej Sołtan Institute for Nuclear Studies, 05-400 Świerk-Otwock, Poland

ARTICLE INFO

Article history:
Received 23 October 2009
Received in revised form 12 March 2010
Accepted 12 March 2010
Available online 21 March 2010

Keywords:
Metals and alloys
Muon spectroscopies
Scanning electron microscopy
X-ray diffraction
Cr_3Si

ABSTRACT

$Cr_{3-x}Co_xSi$ alloys were studied using muon spin relaxation (μSR) and scanning electron microscopy (SEM) techniques. The ferromagnetism observed in non-annealed samples is due solely to cobalt precipitates. Majority of cobalt builds into the A15-type of lattice upon annealing and enhances only its paramagnetic susceptibility. Dynamics of muons in the alloys show a nonmonotonic behaviour with temperature in the temperature range between 150 and 200 K. This effect is likely to be due to the localization of the positive muon at specific interstitial positions in the A15 structure.

1. Introduction

Measurements of magnetic properties of $Cr_{3-x}TM_xSi$ where TM is Fe, Co and Ni show a puzzling behaviour. As-cast samples prepared by arc melting technique exhibit weak ferromagnetic behaviour for Fe doping at $x = 0.3$ (and not at $x = 0.02$, 0.1, 0.2) [1], for Co doping at $x = 0.02$, 0.1, 0.2, and not at $x = 0.3$ [1,2]. It was checked that doping with Ni leaves the sample in paramagnetic state (unpublished).

Positive muons may locate at interstitial positions in the crystal structure, and when no electronic magnetic moments are present they are depolarized by the surrounding nuclear magnetic moments. Muons may also diffuse, and their depolarization rate is then reduced by motional narrowing [3]. For these reasons muons serve as an excellent probe to study even weak magnetic properties.

Even for systems as simple as bcc structures quite complex muon dynamics are observed. For example, the studies [4] of Nb showed that the depolarization rate of muons exhibit a two-cusp structure below ambient temperature, while decreasing to zero at high temperatures. This behaviour was explained by the trapping of muons by a large concentration of defects at low temperature (first cusp), detrapping by thermal agitation and motional narrowing, binding to deeper traps at moderate temperatures (the second cusp), diffusion at high temperatures and motional narrowing again [4].

Muon spin rotation experiments were performed on Co-doped Cr_3Si samples to test the origin of ferromagnetic behaviour. Neither oscillations typical for a ferromagnetic matrix in zero external magnetic field experiments nor a minima in the depolarization rate typical for a Lorentzian distribution of the magnetic field typical for disordered magnetic systems were observed [2] for $x < 0.2$. Instead, the shape of the depolarization rate changes systematically with Co concentration and with temperature. This behaviour cannot be explained by static dipolar interactions of muons with nuclear magnetic moments of Co.

The results from experimental investigations carried out for larger Co concentrations ($x = 0.3$, 0.5) are presented. The samples have also been studied by means of scanning electron microscopy. A change of sample properties under annealing and X-ray investigations allows us to formulate a basic explanation of magnetic behaviour and muon dynamics in Co-doped Cr_3Si samples.

2. Samples

The samples were prepared by melting Cr, Co and Si elements in an arc furnace on a water-cooled copper support under an argon atmosphere cleaned by a titanium getter. The X-ray diffraction measurements with Kα radiation of Cu on annealed samples (900 °C

* Corresponding author. Tel.: +48 857457214; fax: +48 857457223.
E-mail address: pzal@alpha.uwb.edu.pl (P. Zaleski).

0925-8388/$ – see front matter © 2010 Elsevier B.V. All rights reserved.
doi:10.1016/j.jallcom.2010.03.119

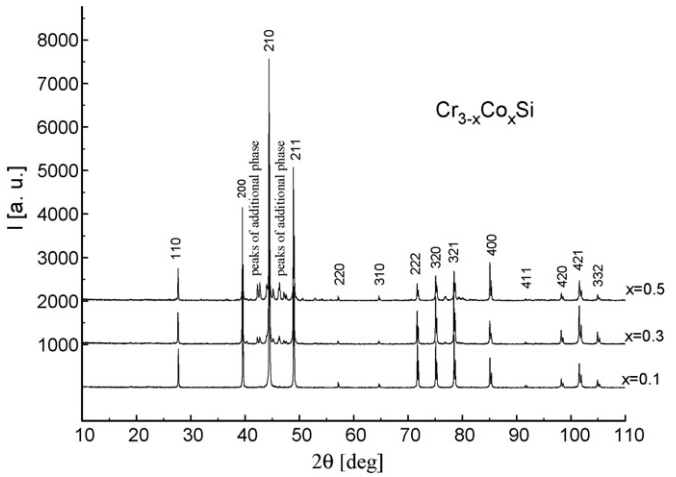

Fig. 1. XRD pattern for samples $x = 0.3$, $x = 0.5$ and $x = 1$ measured with Kα radiation of Cu.

during 24 h) showed that $x = 0.1$ sample is almost a single A15 phase, while additional crystallographic phases could be observed for samples $x = 0.3$ and 0.5 (Fig. 1). Because of small intensity we could not identify the additional phase. The lattice parameters of A15 phase measured for $x = 0.1$, 0.3 and 0.5 are $a = 4.5574\,(1)$, 4.5563 (2) and 4.5556 (4) Å, respectively. The reported value for pure Cr_3Si is $a = 4.555$ Å [5].

The magnetic hysteresis loop previously observed [1] in as-cast samples turned out to disappear after the sample annealing. This is shown in Fig. 2 for the $x = 0.2$ sample which was annealed at 900 °C for 24 h. Magnetization measurements do not show a hysteresis loop down to 10 K. This indicates that ferromagnetism is most likely concerned with cobalt precipitates. When it builds into the lattice of Cr_3Si, the ferromagnetism disappears and the paramagnetic susceptibility shows an increase only. Evidence that cobalt alloys with Cr_3Si for the samples measured is confirmed by the muon spin rotation measurements carried out during this study.

3. Scanning electron microscopy results

The SEM experiment was carried out at Technical University of Białystok using Scanning Microscope Hitachi S-3000N. The samples were polished before SEM experiment. The same samples were used in the μSR experiment (see Section 4) and their images (Fig. 3) show that the samples consist of two phases. X-ray fluorescence measurements indicate that for the $x = 0.3$ sample local compositions are $Cr_{1.91}Co_{1.30}Si_{0.79}$ (light fields in Fig. 3a and c) and $Cr_{3.02}Co_{0.13}Si_{0.85}$ (dark fields in Fig. 3a and c). For the $x = 0.5$ sample compositions are: $Cr_{1.61}Co_{1.45}Si_{0.94}$ (light fields) and $Cr_{2.97}Co_{0.11}Si_{0.92}$ (dark fields) (Fig. 3b and d).

The fractions of light to dark fields in SEM images were estimated by the standard procedure of covering them with a regular grid and counting how many grid elements belong to each fraction. The result is that light fields occupy (9.2 ± 0.9)% of the sample volume for $x = 0.3$ and (22 ± 2)% in the case of the $x = 0.5$ sample.

SEM images of the $x = 0.3$ and 0.5 samples do not change after annealing (900 °C 24 h), see Fig. 3c and d. SEM image of $x = 0.1$ is shown in Fig. 3e for comparison: no patterns of dark and light fields are seen. The measured composition of this sample is $Cr_{2.93}Co_{0.12}Si_{0.95}$. The change in the contrast in Fig. 3e, as well as presence of black spots in Fig. 3a–d, is not correlated with local composition and corresponds to the surface morphology only.

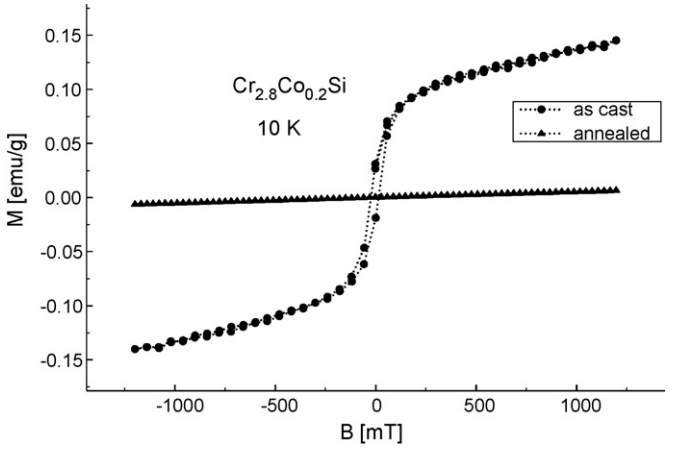

Fig. 2. Magnetization curves of as-cast and annealed (900 °C during 24 h) $x = 0.2$ samples.

4. μSR experiment

The μSR experiment was carried out using the MUSR beam line at the ISIS muon facility, located at the Rutherford Appleton Laboratory in the UK. The μSR technique involves implantation of ~4 MeV 100% spin polarized positive muons, into the first few hundred micrometers of the sample. The interaction of the muon magnetic moment with the local magnetic field H_{loc} results in a precession with the Larmor frequency $\omega_\mu = \gamma_\mu H_{loc}$, where γ_μ is the gyromagnetic ratio of the muon ($2\pi \times 136$ kHz/mT). Having a half-life time $t_{1/2} = 2.2$ μs, most of the muons decay in the first microseconds after the implantation, each of them emitting a positron preferentially in the direction of the muon spin at the time of decay. Evolution of the total muon spin polarization is measured by positron detectors positioned upstream (forward) and downstream (backward) relative to the sample position. The decay asymmetry, $A(t)$, can be defined as follows:

$$A(t) = \frac{N_F(t) - \alpha N_B(t)}{N_F(t) + \alpha N_B(t)} \quad (1)$$

where N_F and N_B are the instantaneous number of events in the forward and backward detectors at time t, and α is a setup-dependent correction factor. From $A(t)$ information about H_{loc} can be deduced.

The as-cast samples were cut into slices and put on a silver holder mounted in helium cryostat. The surface of the holder was not fully covered by the sample, so a fraction of the muon beam was implanted into silver. In order to estimate the fraction of muons stopping in the $x = 0.3$ sample, an experiment in external transverse magnetic field 2 mT using a holder made of Fe_2O_3 was carried out. The muon spin rotation spectrum of Fe_2O_3 has an asymmetry equal to zero because of the fast depolarization rate in the large local magnetic fields. In the case of silver, very small nuclear dipolar magnetic fields exist, so the muon spins may rotate under influence of the external magnetic field only. Therefore two spectra were measured, the first for sample located on the hematite holder, and next for a silver plate with size about 7 cm × 5 cm located on the same hematite holder. The results of these measurements are shown in Fig. 4a. The amplitudes of the measured spectra are (0.19 ± 0.01) in the $x = 0.3$ sample case, and (0.26 ± 0.01) when the measurements are performed for silver. These ratios show that the fraction of muons which stop in the sample is 73 ± 7%. The value of external transverse magnetic field in this experiment was large enough and the internal magnetic field at the muon sites practically does not contribute to the muon depolarization. Additional confirmation of this fact is shown in Fig. 4b. Spectra of the $x = 0.3$ sample on the Ag holder and Ag holder itself measured in transverse field 0.2 mT show similar asymmetry. Therefore there are no

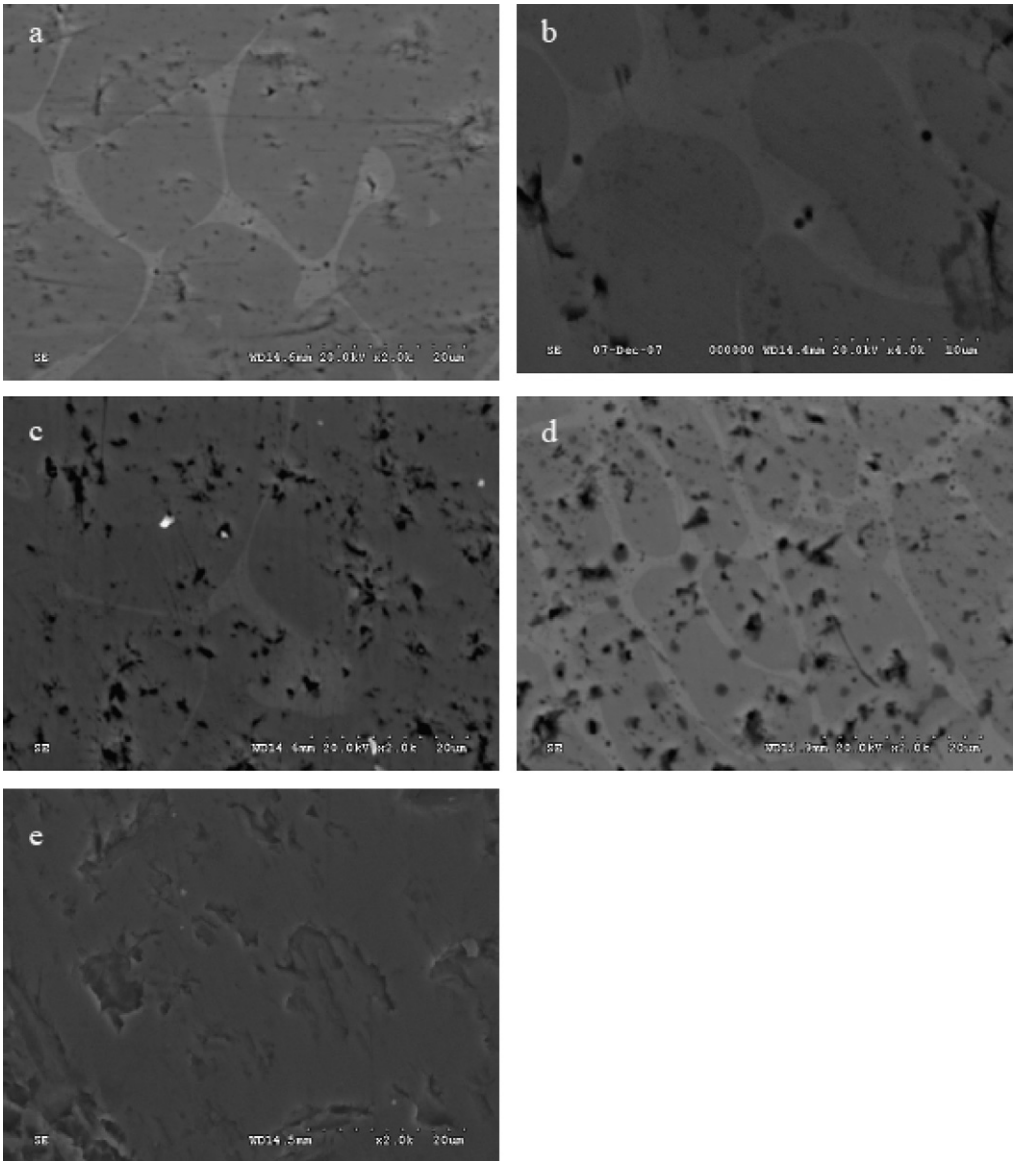

Fig. 3. Images from SEM: (a) for as-cast $x = 0.3$ sample, (b) for as-cast $x = 0.5$ sample, (c) for annealed $x = 0.3$ sample, (d) for annealed $x = 0.5$ sample, (e) for as-cast $x = 0.1$ sample. The focus on the image (b) is two time greater than in other.

large internal fields at the muon site in the sample. All samples were measured in zero external magnetic field in the temperature range 10–400 K. Typical spectra for the $x = 0.5$ sample are shown in Fig. 5. A systematic increase of the depolarization rate is observed as the temperature is reduced from 400 to 200 K (Fig. 5). This can be easily understood in terms of a reduction in the hopping rate with temperature. However, rather unexpected decrease of the depolarization rate (especially for $x = 0.3$), see Fig. 6 appears between 200 and 100 K. Possible mechanism for such behaviour will be discussed in the following sections.

5. Analysis of μSR experiment

The interpretation of previously measured depolarization rate in $Cr_{3-x}Co_xSi$ with $x = 0$, 0.1 and 0.2 was presented in [2], and was quantitatively explained by the interaction of muon spins with Co nuclear dipolar fields and by the muon diffusion.

The quantitative spectra analysis was performed within the framework of the model proposed by Hayano et al. [6]. In this model one assumes a Gaussian distribution of the internal magnetic fields and a certain frequency of muon jumps between lattice positions. Internal field dynamics, resulting either from muon hopping from site to site or from the fluctuating internal fields, can be accounted for within the strong collision approximation [7]. This approximation is based on two assumptions. The first is that the local field changes its direction at a time t according to a probability distribution $p(t) = \exp(-\nu t)$; $\nu = 1/\tau$ where τ is correlation time of the field fluctuation. The second is that the field after such a "collision" is chosen randomly from the distribution $P(H_{loc})$ and is entirely uncorrelated with the field before the collision; H_{loc} is the internal field.

Because of the presence of fraction of muons with a small depolarization rate (among them the fraction implanted in the Ag holder), a linear combination of a Dynamic Kubo–Toyabe function ($G_z^{DKT}(t)$) [6] and a non-relaxing fraction was fitted to the experimental data:

$$G(t) = A + BG_z^{DKT}(t) \quad (2)$$

where A and B are constants. Parameters A and B are linearly dependent, the sum of A and B is equal to asymmetry at $t = 0$.

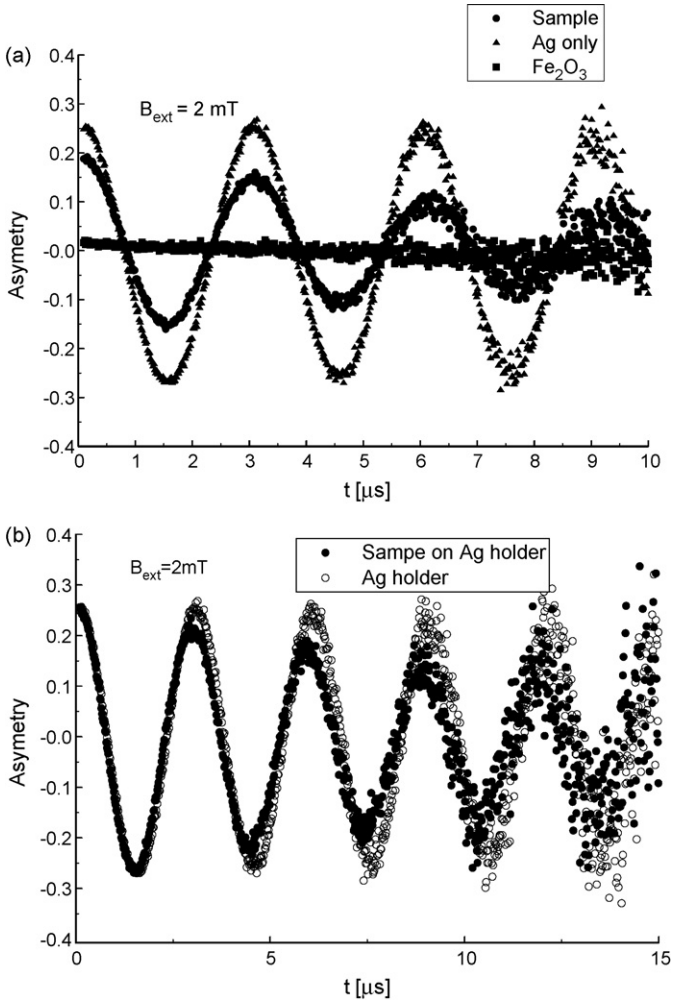

Fig. 4. (a) Spectra of Fe_2O_3, sample $x = 0.3$ attached to Fe_2O_3 plate, and Ag holder attached to Fe_2O_3 plate, (b) spectra of $x = 0.3$ sample on Ag holder and Ag holder itself measured in external transverse field 2 mT.

Representative examples of fits of (2) are shown by solid lines in Fig. 6. The width of Gaussian distribution and frequency of diffusion jumps at selected temperatures obtained from fits are shown in Table 1 (previously measured results [2] for $x = 0$, 0.1, 0.2 are also included for consistency). A systematic increase of the width of the distribution Δ and decrease of the jump rate with Co concentration are obtained. The good quality fits can be obtained only when both parameters Δ and ν are free during the fitting procedure.

Table 1
(a) Width of Gaussian distribution [in mT] and (b) jump rate [in MHz] for $Cr_{3-x}Co_xSi$ samples.

	5 K	100 K	200 K	300 K	400;K
(a)					
$X = 0$	0.16 ± 0.01	0.11 ± 0.01	0.06 ± 0.01	0.05 ± 0.01	0.06 ± 0.02
$X = 0.1$	0.78 ± 0.30	0.30 ± 0.02	0.21 ± 0.02	0.24 ± 0.02	0.22 ± 0.03
$X = 0.2$	0.40 ± 0.01	0.35 ± 0.02	0.29 ± 0.02	0.33 ± 0.02	0.21 ± 0.02
$X = 0.3$	0.41 ± 0.01	0.41 ± 0.01	0.37 ± 0.01	0.37 ± 0.01	0.30 ± 0.01
$X = 0.5$	0.47 ± 0.01	0.47 ± 0.01	0.41 ± 0.01	0.40 ± 0.01	0.34 ± 0.01
(b)					
$X = 0$	30.0 ± 1.0	19.3 ± 1.0	7.5 ± 7.5	7.5 ± 7.5	15.0 ± 1.0
$X = 0.1$	16.0 ± 2.0	15.5 ± 1.5	7.6 ± 1.5	9.6 ± 1.5	15.3 ± 1.7
$X = 0.2$	10.0 ± 0.5	9.3 ± 1.2	4.4 ± 0.5	5.9 ± 1.0	7.3 ± 1.0
$X = 0.3$	1.34 ± 0.06	2.04 ± 0.06	3.97 ± 0.06	4.16 ± 0.06	5.48 ± 0.06
$X = 0.5$	1.23 ± 0.06	2.18 ± 0.06	3.22 ± 0.06	3.26 ± 0.06	6.47 ± 0.06

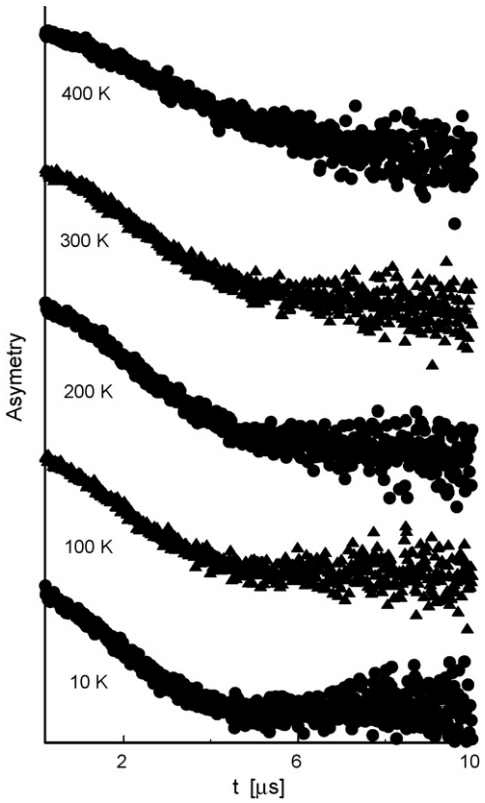

Fig. 5. Spectra for $x = 0.5$ sample measured at different temperatures.

Before going to more advanced quantitative analysis, a function containing a stretched exponential:

$$G = A + B\ e^{-(\lambda t)^{\beta}} \tag{3}$$

was fitted to the measured spectra. In Eq. (3) β were chosen as a constant for given x, and λ and A were free, temperature dependent parameters. The value of the parameters β for given x were adjusted as the averages taken from pre-fits with all free parameters and amount to 2.78 for $x = 0.3$ sample and 1.99 for $x = 0.5$ sample. The fits revealed that the temperature dependence of the depolarization rate occur for both samples ($x = 0.3$ and 0.5). It is nonmonotonic at the same temperature range, see Fig. 7 in which previously measured results [2] for $x = 0.1$ and $x = 0.2$ are also included. A similar temperature behaviour is observed for constant A, see Fig. 8. The most pronounced nonmonotonic behaviour of A is observed for $x = 0.3$. It can also be easily seen in Fig. 6.

6. Estimation of static distribution of nuclear dipolar interactions

Muons are likely to localize at interstitial positions of metallic crystals. In the A15 structure there are only three nonequivalent interstitial positions shown in Fig. 9, abbreviated by X, Y and Z. Each one is formed by four atoms at corners of nonregular tetrahedron. Interstitial position Z located at the main diagonal with coordinates $(\xi, \xi, \xi)a$, where $\xi = 5/24 = 0.208$ is of particular interest. For these interstitials, the distance to the four neighbouring atoms (1Si, 3Cr) is $5/24 \times 3^{1/2}a = 0.361a$, the largest distance to the four atoms in the A15 structure. In the unit cell there are four Z-type interstitial positions located at main diagonal with coordinates ξ, $1/2 \pm \xi$, $1 - \xi$. The interstitial positions with coordinates ξ and $1/2 - \xi$ are located close to each other and the five corner atoms (2Si and 3Cr) of these positions form a cage (see Fig. 9) which is a candidate for muon location.

Table 2
Properties of interstitial positions in A15 structure; a is lattice parameter; convention for coordinate (column 2) is that Si is at (0, 0, 0) position in the cubic unit cell.

Interstitial position	Coordinates	Distance to nn atoms	nn atoms in Cr_3Si	$a^6\sum^{\infty}1/r^6$ for Cr sublattice	$a^6\sum^{\infty}1/r^6$ for Si sublattice
X	5/32 (2, 1, 0) a	$\frac{5\sqrt{5}}{32}a$	3Cr, 1Si	1829	605.4
Y	1/4 (2, 1, 0) a	$\frac{\sqrt{2}}{4}a$	4Cr	2157.2	146.5
Z	5/24 (1, 1, 1) a	$\frac{5\sqrt{3}}{24}a$	3Cr, 1Si	1545.3	539.9

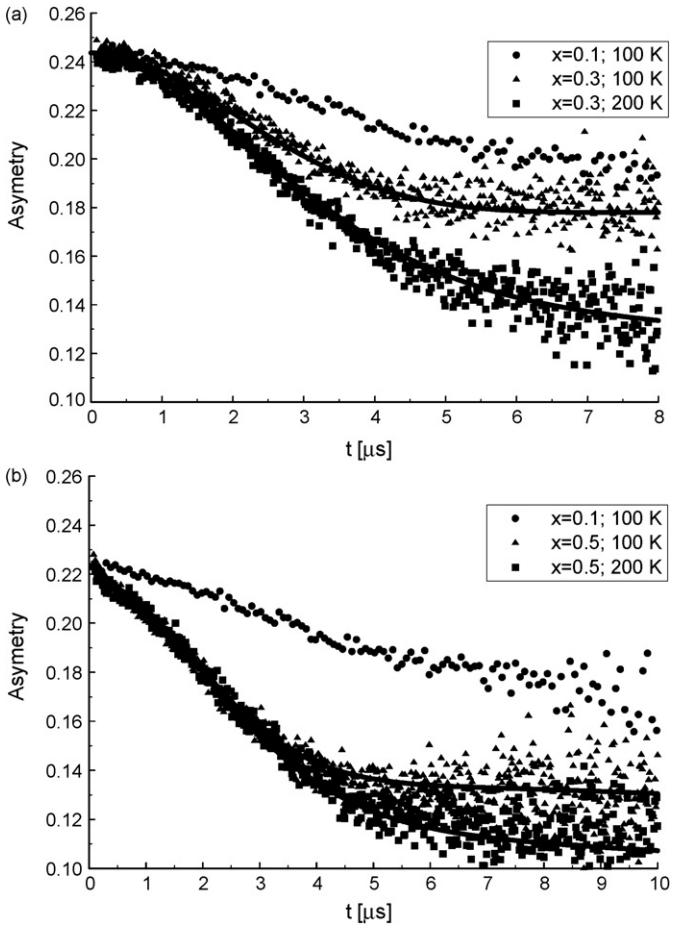

Fig. 6. μSR spectra for samples $x = 0.1$, $x = 0.3$ (a) and $x = 0.5$ (b). Solid lines show typical fits, see Eq. (2). Spectrum of $x = 0.1$ sample is shown for comparison.

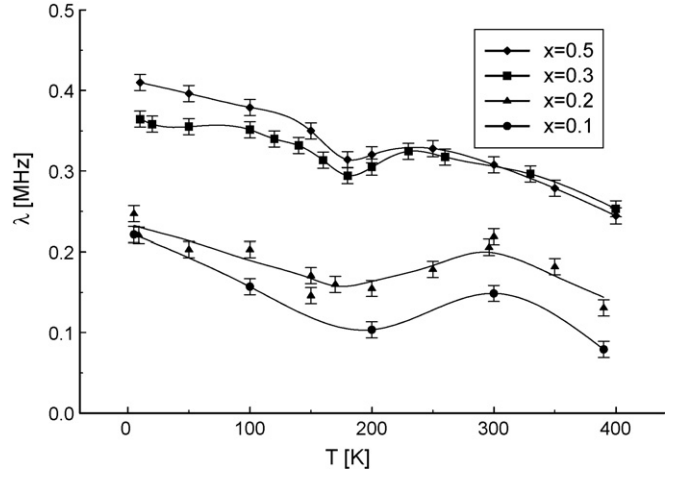

Fig. 7. The temperature dependence of depolarization rate (see Eq. (3)) for sample $x = 0.3$ and 0.5. The lines are guides for the eyes only.

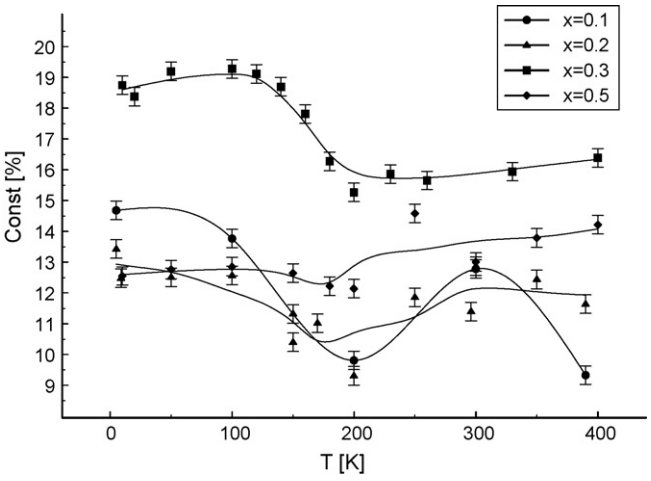

Fig. 8. Values of the constant A in $Cr_{3-x}Co_xSi$ alloys (see Eq. (3)). The lines are guides for the eyes only.

Other interstitial positions are characterised in Table 2 and shown in Fig. 9. The width of the Gaussian distribution was calculated for the various interstitials using formula [6,8]:

$$\Delta_{KT} = \sqrt{\sum_j c_j \ \Delta_{KT}^2(j)} \tag{4}$$

where

$$\Delta_{KT}^2(j) = \left(\frac{\mu_0}{4\pi}\right)^2 j(j+1)\gamma_j^2\gamma_\mu^2\hbar^2\frac{4}{9}\left(1+\frac{3}{8}\frac{j+1/2}{j(j+1)}\right)\sum_{i=1}^{\infty} r_i^{-6} \tag{5}$$

The coefficient c_j is the weight depending on the concentration of elements in the given phase and natural isotopic abundance. The parameters in (4) and (5) are: j – nuclear spin of the elements, γ_j

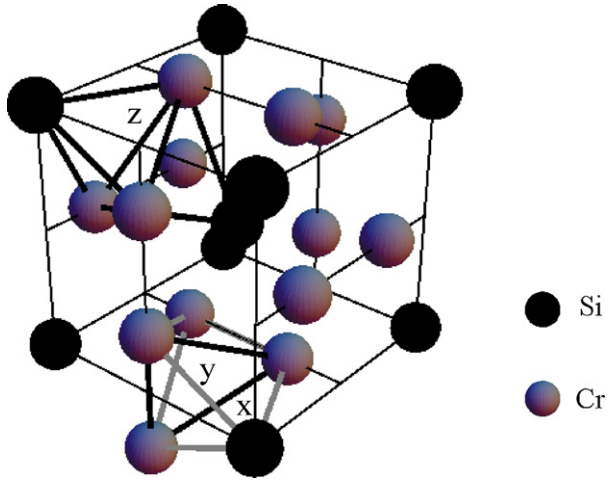

Fig. 9. Interstitial positions in A15 Structure.

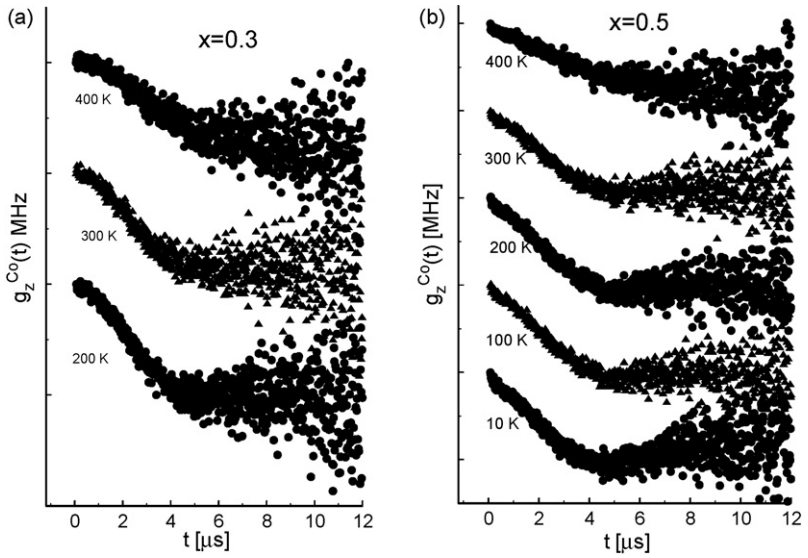

Fig. 10. $g_z^{Co}(t)$ spectra extracted of Co-rich phase (see Eq. (8)) for $x = 0.3$ sample (a) and $x = 0.5$ sample (b).

– nuclear gyromagnetic ratio, r_i – the distance between interstitial position and the lattice site i. The formula (4) enables Δ_{KT}^2 to be determined for each sublattice (Cr, Si, and Co). The value of expression $a_0^6 \sum_i^{\infty} r_i^{-6}$ for all different interstitial positions (Fig. 9) for the A15 structure are collected in Table 2. The calculated widths of the distribution for $x = 0.1$ sample with the A15 structure are collected in Table 3.

7. Estimation of the depolarization rate in Co-rich phase

SEM results for Cr rich phases in both $x = 0.3$ and $x = 0.5$ samples indicate that their composition is close to that of $Cr_{3-x}Co_xSi$ with $x = 0.1$. This rather accidental result permits an estimation of the depolarization rate of the Co-rich phase. It follows from Section 4 that $1 - s$ fraction of the muon beam hits the sample, while s fraction of the beam hits the silver plate. The depolarization rate of muons stopping in silver holder is negligible. Thus the observed asymmetry for the $x = 0.1$ sample is

$$A^{Cr}(t) = A_0(s + (1-s)g_z^{Cr}(t)) \tag{6}$$

where $g_z^{Cr}(t)$ is the zero field relaxation function of Cr rich phase and A_0 is a setup related experimental factor corresponding to the asymmetry at time $t = 0$. The $x = 0.3$ sample, may be regarded as fraction $(1 - c)$ of Cr rich sample (dark fields in Fig. 3a and c) and fraction c of the Co-rich phase (light fields in Fig. 3a and c), whose zero field longitudinal relaxation function is $g_z^{Co}(t)$. Thus the observed asymmetry for both the $x = 0.3$ and $x = 0.5$ samples may be approximated by:

$$A^{Co}(t) = A_0(s + (1-c)(1-s)g_z^{Cr} + c(1-s)g_z^{Co}(t)) \tag{7}$$

Table 3
Width of the field distribution [mT] calculated for various interstitial position for $x = 0.1$ sample.

	$Cr_{2.9}Co_{0.1}Si$
X	0.159
Y	0.170
Z	0.146

From the Eqs. (6) and (7) $g_z^{Cr}(t)$ may be eliminated and $g_z^{Co}(t)$ is

$$g_z^{Co}(t) = \frac{A^{Co}(t) - (1-c)A^{Cr}(t)}{A_0 c(1-s)} - \frac{s}{1-s} \tag{8}$$

The values of the function $g_z^{Co}(t)$ should be between 1 and 0. It was possible to estimate the shape of $g_z^{Co}(t)$ using $c = 0.38$ and $s = 0.2$ for the $x = 0.5$ sample at all temperatures, see Fig. 10. The procedure fails for the $x = 0.3$ sample because the content of the Co-rich phase is small. The dynamic Kubo–Toyabe function was fitted to the estimated $g_z^{Co}(t)$ spectra. The width of distribution and the jump rates are shown in Figs. 11 and 12, respectively. The width of the distribution of the Co-rich component $g_z^{Co}(t)$ is systematically larger than the width of the whole $x = 0.5$ sample, as expected. Interestingly, the nonmonotonic behaviour shown in Fig. 11 is not as pronounced as those shown in Fig. 14. This observation suggests that nonmonotonic behaviour relates rather to the A15 phase and not to the Co-rich phase.

8. Discussion

Initially [2] μSR experiments in Co-doped Cr_3Si were motivated by the detection of a small magnetization in the $Cr_{3-x}Co_xSi$ host. The

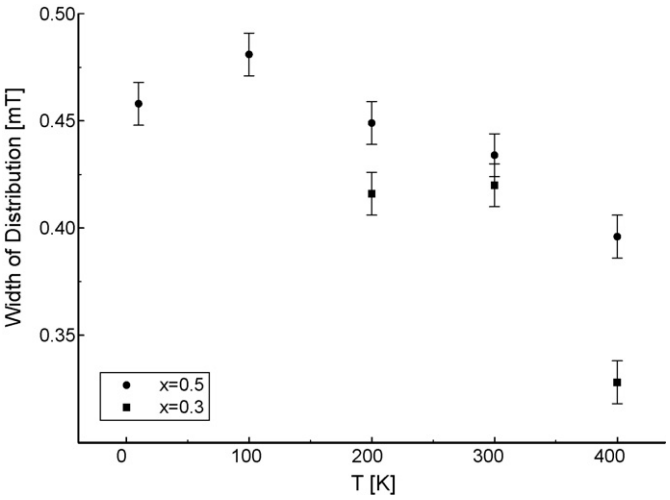

Fig. 11. Width of field distribution fitted for $g_z^{Co}(t)$.

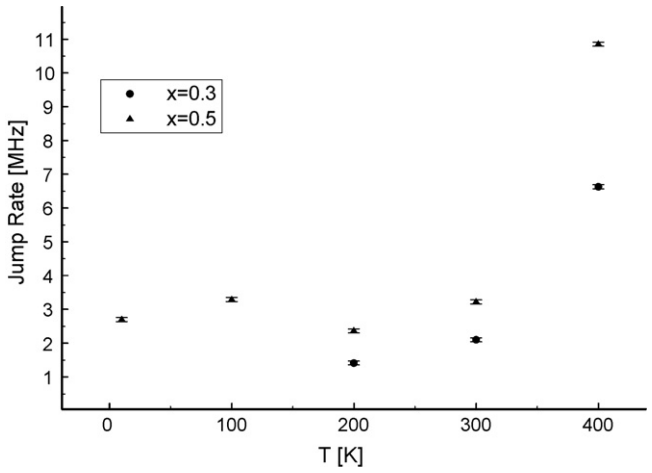

Fig. 12. Jump rate fitted for $g_z^{Co}(t)$.

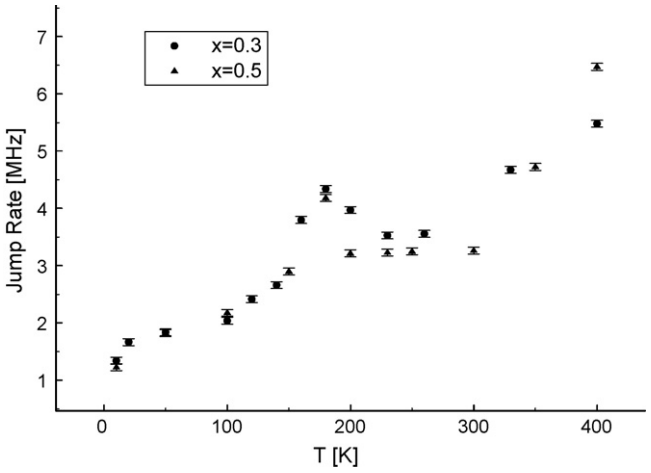

Fig. 13. Jump rate in $Cr_{3-x}Co_xSi$ alloys.

experiments performed on samples with $x = 0$ and 0.1 revealed that the muon depolarization rate can be explained by nuclear dipolar fields alone, and we were therefore able to exclude the presence of electronic type magnetization in the host. However, the as-cast samples with $x = 0.02$, 0.1 and 0.2 show a nonzero magnetization, while the sample with $x = 0.3$ exhibits zero magnetization. To the best of our knowledge, the ternary phase diagram Cr–Co–Si is not known, and therefore results of SEM are of key importance for explaining the observed behaviour. The binary Cr–Si phase diagram shows a relatively narrow region where a single A15 phase is formed [9]. The width depends on temperature and is about 5% of the concentration range. When a small amount of Cr is replaced by Co, we may still expect that a single A15 phase is formed. During crystallization of Cr–Co–Si A15 phase from the melt, a small amount of Co_3Si may precipitate because of its low melting temperature (1960 K for Cr_3Si and 1483 K for Co_3Si) [9]. Below $T = 1467$ K Co_3Si is unstable and decomposes to ε-Co and α-Co_2Si [9]. The fraction of these phases is so small that they are not detected by X-ray diffraction and in SEM experiment. Because ε-Co is ferromagnetic, these inhomogeneities are detected by the magnetization measurement. Annealing causes homogenization of the sample and ferromagnetic regions disappear via diffusion processes.

For larger Co concentrations in the $Cr_{3-x}Co_xSi$ system, $x > 0.2$, we enter into a thermodynamically stable two phase region, seen clearly by the SEM images and the X-ray diffraction pattern. During crystallization from the melt in the two phase region, a typical dendrite structure of approximate composition $Cr_{3-x}Co_xSi$ $x \approx 0.1$ is initially formed, while the remaining liquid finally forms the other crystallographic phase rich in Co. The candidate for the structure of the second phase seen as the light fields in Fig. 3a–d is Co_2Si [9] with part of Co substituted by Cr, or $Cr_5Co_3Si_2$ [10]. Both Co_2Si and $Cr_5Co_3Si_2$ are not ferromagnetic and their presence probably prevents formation of ε-Co inhomogeneities.

Although the muon relaxation spectra of measured samples changes systematically with temperature and concentration, their shapes cannot be regarded as rich in information. One may doubt that postulating the model (2) and performing a fit with three free parameters (jump rate, width of the Gaussian distribution and a constant), which usually are strongly correlated, it is possible to be convinced that muon dynamics change at a certain temperature. Previously [2] we tried to interpret data using the simplest physical picture, essentially postulating that the nuclear dipolar field distribution is constant and that the jump rate increases with temperature. The most convincing result showing that we observe some nonmonotonic behaviour of the depolarization rate is presented in Fig. 7. Parameterization is done by variation of two parameters only. Thus we are also convinced that nonmonotonic jump rate presented in Fig. 13 corresponds to physical processes and not to mathematical artefact.

The hop rate, ν, of the muon is of the order of MHz. During its half-life time $t_{1/2}$, of the order of μs, muon performs about $\nu t_{1/2}$ diffusion jumps. Assuming that it is random walk, muon travels an average distance of $a(\nu t_{1/2})^{1/2}$, which is of the order of 7–18 Å. Thus it is unlikely that a significant fraction of muons diffuse from one crystallographic phase to another. Some important information can be extracted from the temperature dependence shown in Figs. 7, 8, 13 and 14. We observe clear anomalies for the $x = 0.3$ and $x = 0.5$ samples and a less pronounced nonmonotonic behaviour for $x = 0.1$ and $x = 0.2$ (Figs. 7 and 8) over the same temperature range. Also, the most pronounced nonmonotonic behaviour of muon dynamics (Figs. 7, 8, 13 and 14) is observed for sample $x = 0.3$ and not for $x = 0.5$. This suggests that anomalous behaviour is rather a property of the $Cr_{3-x}Co_xSi$ system with the A15 structure and depends on Co concentration. This conclusion is consistent with results of the analysis of Co-rich phase performed in the previous section.

Experiments indicate some similarity between the behaviour shown in Fig. 6 and that discussed in the introduction [4]. At $T = 200$ K the muon depolarization rate is smaller than at $T = 100$ K. One possible explanation is that mobile muons at $T = 100$ K are trapped by a low concentration of traps lower in energy than traps at interstitial positions.

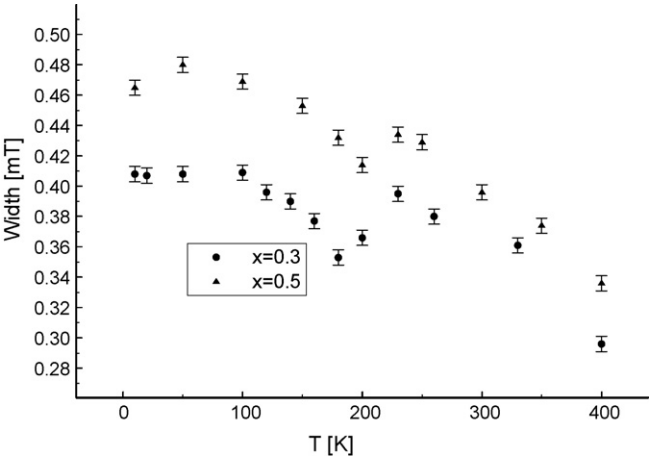

Fig. 14. Width of the Gaussian distribution of magnetic field in $Cr_{3-x}Co_xSi$ alloys.

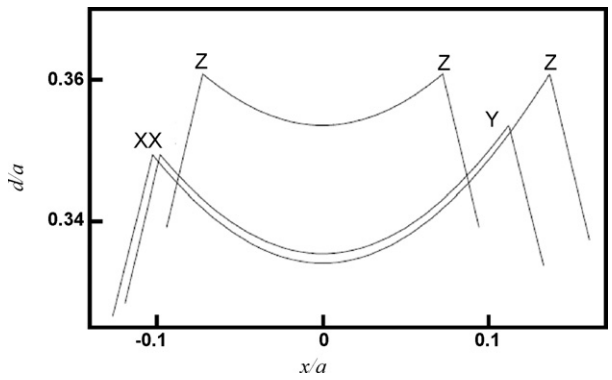

Fig. 15. Geometrical properties of interstitial position in the A15 structure, where x is the coordinate on the line connecting centers of two nearest interstitial positions (see Table 2), d is the distance between the point with coordinate x and the nearest atom, a is unit cell size. Zero of the x coordinate was set at the minimum of d/a.

Another possibility can follow from the specific structure of the investigated system; as discussed earlier, a pair of Z-type of interstitial positions form a prism or *Z–Z* cage, see Fig. 9. From Fig. 15 it is clear that because of geometrical reasons, the *Z–Z* cage is a candidate muon localization; however within this cage the muon may form a coherent state or may perform fast vibrations between two Z-type interstitial positions. In each case the dipolar field sensed by muon spin in the *Z–Z* cage is averaged and is smaller than the local fields in the *X* and *Y* or *Z* interstitial positions. This behaviour – resulting in a decrease of the depolarization rate – will result in an effective change of the constant *A* in the fitted function, since Eq. (2) is just an approximation and not a precise description of the muon dynamics. When the temperature is raised to approximately 200 K localized *Z–Z* states are excited and the muon also jumps between *X*, *Y* and *Z* interstitial positions. The frequency of jumps is much smaller than the frequency of vibrations in the *Z–Z* cage and thus the depolarization rate increases.

Although systematic changes of the width of the static magnetic field distribution with temperature (Fig. 14) are observed, this is most probably a result of the simplification used in (2) for the description of the complicated muon dynamics. More important, however, the widths obtained for the series of $Cr_{3-x}Co_xSi$ up to $x = 0.5$ show, on average a similar trend to the estimated widths. A similar trend to the estimated widths of the static dipolar fields. The widths of the field distribution estimated at different temperatures are collected together in Fig. 16. The values obtained from fits (Eq. (2)) show a clear dependence on x and are systematically larger than the results of an estimation based on Eq. (4). This effect can arise from strong correlation between the width Δ_{KT} and jump rate ν. Indeed, an increase of Δ_{KT} will result in an increase of the depolarization rate, while an increase of the jump rate ν results in a decrease of the depolarization rate. If the spectra are flat, the increase of Δ_{KT} can be compensated by an increase of the jump rate, ν, resulting in a similar shape of the fitted function.

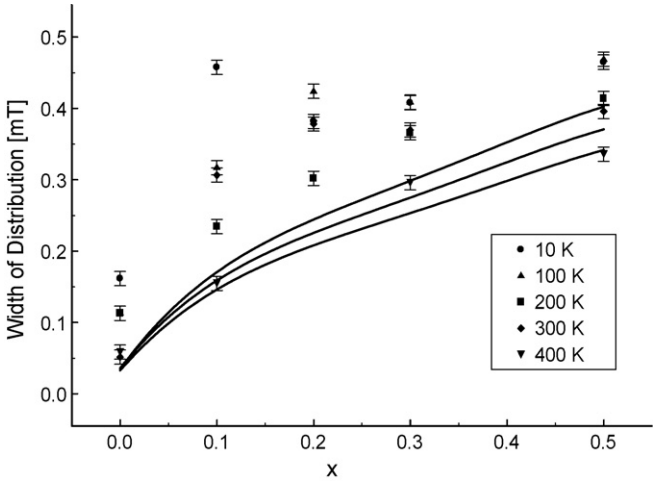

Fig. 16. Widths of the Gaussian field distribution estimated from fits (Eq. (8)) at different temperatures. The lines correspond to the width of the Gaussian field distribution at three different interstitial sites (*X*, *Y*, and *Z*) in the Cr_3Si resulting from nuclear dipolar interactions (Eq. (4)).

Naturally the questions arise about the possibility of fitting the spectra by applying constraints to Eq. (2) and keeping constant the width of the distribution and parameter *A*, changing only the frequency of the diffusion jumps. We could not obtain, however, fits of good quality under such assumptions. The expression (2) is thus the effective description of the observed spectra, although this does not contain details of the muon dynamics as described for example in [4].

9. Conclusions

The ferromagnetic properties of as-cast samples with $x \leq 0.2$ are explained by the presence of Co-rich impurities originating from ε-Co. Sample annealing leads to formation of a regular $Cr_{3-x}Co_xSi$ alloy. The μSR experiment performed on paramagnetic samples with $x = 0.3$ and 0.5 shows anomalies in muon dynamics. The presence of a nonmonotonic behaviour was demonstrated by fitting the stretched exponentials and dynamic Kubo–Toyabe functions. The existing nonmonotonic behaviour over the same temperature excludes artefacts caused by correlation between parameters. A clear cusp in the jump rate is observed in the temperature range 150–200 K for $x = 0.3$ and 0.5 samples. Muon experiments with Fe_2O_3 enable an estimation of the shape of muon depolarization rate for Co-rich crystallographic phase. It was argued that nonmonotonic behaviour is rather property of A15 phase and not Co-rich phase detected in $x = 0.3$ and 0.5 samples by X-ray and SEM techniques. The nonmonotonic behaviour of the jump rate is interpreted as the trapping of muons at moderate temperatures (150–200 K). It is suggested that a possible trap for the positive muon is the *Z–Z* cage. A systematic decrease of muon jump rate ν with increase of Co concentration x is observed.

References

[1] P. Zaleski, M. Biernacka, L. Dobrzyński, K. Perzyńska, K. Rećko, Phys. Stat. Sol. (a) 196 (1) (2003) 260–262.
[2] P. Zaleski, K. Szymański, M. Biernacka, S. Cottrell, K. Perzyńska, K. Rećko, L. Dobrzyński, J. Alloys Compd. 442 (2007) 213–215.
[3] A. Schenck, in: J.B. Warren (Ed.), Nuclear and Particle Physics at Intermediate Energies, Plenum, New York, 1976.
[4] C. Boekema, R.H. Heffner, R.L. Hutson, M. Leon, M.E. Schilaci, W.J. Kossler, M. Numan, S.A. Dodds, Phys. Rev. B 26 (1982) 2341.
[5] H.P.J. Wijn, Magnetic Properties of Metals, d-Elements, Alloys and Compounds, Springer-Verlag, Berlin, Heidelberg, 1991, p. 146.
[6] R.S. Hayano, Y. Uemura, J. Imazato, N. Nishida, T. Yamazaki, R. Kubo, Phys. Rev. B 20 (1979) 850.
[7] R. Kubo, J. Phys. Soc. Jpn. 9 (1954) 935.
[8] A. Seeger, Hyperfine Interact. 17–19 (1984) 75.
[9] B. Massalski, Binary Alloy Phase Diagrams, 2nd ed., ASM International, Materials Park, OH, 1990.
[10] E.I. Gladyshevskii, P.I. Kripyakevich, Yu.B. Kuz'ma, Trans. Zhurnal Strukturnoi Khimii 3 (1962) 414.